# Three-Dimensional Quantitative Analysis of Hemispheric Asymmetry in the Human Superior Temporal Region

William C. Loftus,[1] Mark Jude Tramo,[2] Catherine E. Thomas,[1] Ronald L. Green,[3] Robert A. Nordgren,[1] and Michael S. Gazzaniga[1]

[1]Center for Neuroscience, University of California, Davis, California 95616, [2]Department of Neurobiology, Harvard Medical School, and Neurology Service, Massachusetts General Hospital, Boston, Massachusetts 02115, and [3]Department of Psychiatry, Dartmouth Medical School, Hanover, New Hampshire 03755

**The recent observations of overall symmetry of the caudal infrasylvian region by Steinmetz et al. (1990) and Witelson and Kigar (1991, 1992) diverge from earlier findings of leftward asymmetry in this region (Geschwind and Levitsky, 1968; Galaburda et al., 1987; Larsen et al., 1989). To address this inconsistency, we measured the entire infrasylvian surface posterior to Heschl's gyrus from coronal magnetic resonance images of 10 young, normal, right-handed subjects. Computer models were constructed by tracing contours of this region and then interpolating a 3D triangle mesh between each pair of adjacent contours. Measurements of these models showed no significant directional asymmetry. The same contour set was used to obtain measurements with a conventional algorithm that does not interpolate a surface between contours. The results obtained with the second method showed significant leftward asymmetry. These results suggest that in some cases, unbalanced distortions due to folding differences of the hemispheres are sufficient to obtain spurious findings of left–right asymmetry. This supports the claim of Steinmetz and Witelson that leftward asymmetry is restricted to the temporal bank of the caudal infrasylvian surface, and is balanced by rightward asymmetry of the parietal bank.**

Neural systems within the superior temporal region of the left hemisphere mediate language perception and cognition in the vast majority of humans. Evidence that the putative language area of Wernicke (1874) resides in the caudal extent of this region has been accrued primarily through lesion localization studies in patients with aphasia (for review, see Nass and Gazzaniga, 1987). Hemispheric size asymmetries (left greater than right) involving the superior temporal region of postmortem specimens were first described in the German literature in the early part of this century and first quantified by Geschwind and Levitsky 25 years ago. These findings have been replicated in subsequent postmortem (Teszner et al., 1972; Witelson and Pallie, 1973; Wada et al., 1975; Chi et al., 1977a,b; Galaburda et al., 1987; Larsen et al., 1989; Steinmetz et al., 1989) and *in vivo* studies (Larsen et al., 1990; Steinmetz et al., 1991; Leonard et al., 1992) and have been reported by some investigators to include that part of the supramarginal gyrus lying along the inferior bank of the posterior ascending sylvian ramus (PAR). The results have been interpreted as anatomical evidence that Wernicke's area resides in this region. However, the proportion of individuals in whom the left is larger (e.g., 65% in Geschwind and Levitsky's series) is considerably less than that estimated for left hemisphere language dominance in the general population (approximately 90–95%; for review, see Witelson, 1977).

One interpretation of the findings of left–right asymmetry is that they reflect a left hemisphere advantage with respect to cortical surface area in the posterior language region. On the other hand, it has also been suggested that these findings hinge on focusing strictly on the planum temporale (PT) (see below), whose asymmetry may be due to hemispheric differences in folding patterns and arbitrary anatomic delineations in the posterosylvian region (Rubens et al., 1976). Two recent studies have found no size asymmetries involving the full extent of the caudal infrasylvian surface (cIS) (Steinmetz et al., 1990; Witelson and Kigar, 1991, 1992) comprising both the PT and infrasylvian supramarginal gyrus, yet these results differ with previous findings of leftward asymmetry even when the supramarginal portion is included (Geschwind and Levitsky, 1968; Witelson and Pallie, 1973; Galaburda et al., 1987; Larsen et al., 1989, 1990). Steinmetz et al. (1990) speculated that in these cases, asymmetry may be accounted for by more pronounced

photographic foreshortening in the right hemisphere, but such distortions have never been measured explicitly. The purpose of this article is to (1) propose a 3D method of measuring cortical surface area and apply it to the region comprising the superior temporal gyrus and infrasylvian supramarginal gyrus, and portions thereof; (2) compare this method with the heretofore state of the art method (the "quasi-3D" method) in order to quantify distortions of the latter; and (3) use this new data to shed light on the inconsistencies in the literature regarding left–right (a)symmetry in the posterior language region. The two methods are contrasted in Figures 1 and 2.

## Materials and Methods

### *Subjects*

The magnetic resonance (MR) images of five males and five females with normal neurological and psychiatric histories were analyzed. Each subject was the first-born member of monozygotic twins who had been recruited for another study (M. J. Tramo, W. C. Loftus, C. E. Thomas, R. L. Green, L. A. Mott, and M. S. Gazzaniga, unpublished observations). The age range was 18–43 years with a mean age of 32 years. All subjects were right-handed [Edinburgh Laterality Quotient (Oldfield, 1971): range, 58–100; median, 89]. The Full-Scale Wechsler Intelligence Quotient (Wechsler, 1981) ranged from 87 to 127 with a median of 99.

### *Image Acquisition*

T1-weighted MR images were acquired in the coronal plane (section thickness, 3.0 mm, no gap) using either a Siemens 1.0 Tesla Magnetom system or a General Electric 1.5 Tesla Signa system that yielded 256 × 256 image matrices with pixel resolutions of 1.17 and 0.937 mm, respectively. In eight subjects, images were obtained via 3D FLASH with TE/TR = 20 msec/400 msec (Siemens) or 9 msec/50 msec (GE). Before this technology became available at our institution, contiguous sections were obtained by interleaving two sets of 3.0 mm sections with 3.0 mm gaps. The head was positioned in the scanner so that a horizontal laser marked the intercanthal line and a vertical laser intersected the midpoint of the nasion and philtrum. Sagittal sections were imaged (slice thickness, 5.0–8.0 mm; gap, 1.0 mm; in-plane resolution, ≤1.07 mm) and inspected for rotational tilt by observing whether the rostrum and splenium of the callosum, optic chiasm, and fourth ventricle were evident on the same (mid-sagittal) image. The images were stored on magnetic tape and transferred to a Silicon Graphics workstation.

### *Anatomical Designations*

The planum temporale (PT) is defined here as the superior surface of the superior temporal gyrus lying caudal to the transverse gyrus(i) of Heschl (HG). This definition corresponds to that of von Economo and Horn (1930) and has recently been employed by Steinmetz et al. (1989, 1990). Its caudal border lies at the point of upward angulation of the posterior

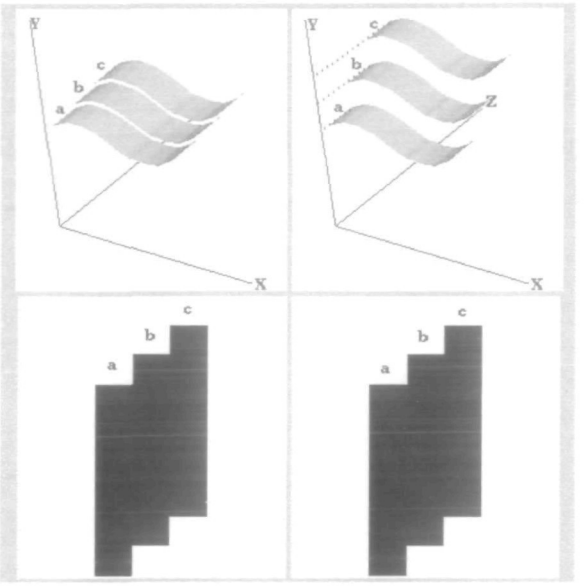


**Figure 1.** The quasi-3D method. In all perspective renderings (Figs 1, 2, 5, 6), the *z-axis* indicates the interslice axis and is pointing away from the viewer; the slice planes are parallel to the *x–y plane*. *Top left*, Three contours (*a–c*) occupying successive positions (e.g., slice positions) along the *z-axis*. Slice thickness is indicated by the width of the "ribbons." Since there is very little difference in elevation (*y-axis position*) among the three contours, the model is oriented nearly parallel to the *x–z plane*. *Top right*, The same contours as on the *left* at the same *z*-positions but with greater disparity in their elevation (indicated by the *dotted lines* projected onto the *y-axis*), resulting in a greater angulation with respect to the *x–z plane*. The surface area of the quasi-3D model is the summed length of the ribbons multiplied by their thickness. Despite the geometric differences, both models have the same surface area. *Bottom left* and *right*, An alternative way of estimating surface area that is equivalent to the quasi-3D method is to measure the area of a 2D map formed by unraveling the ribbons onto a plane. Again, the 2D maps for each set of contours are identical, reflecting the equality of the two models.

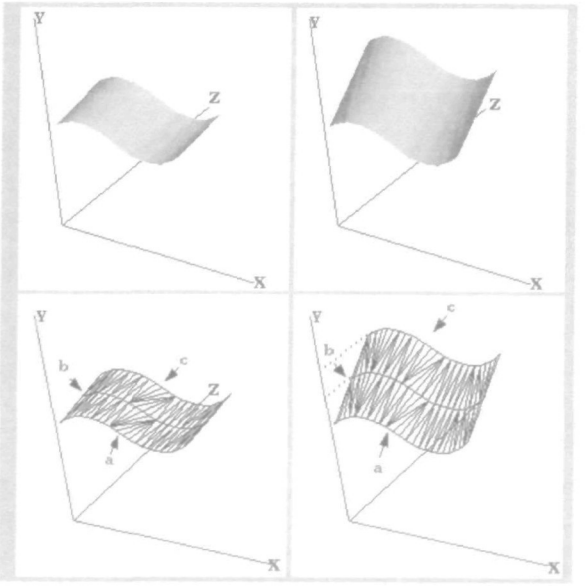


**Figure 2.** The 3D method. *Top*, Shaded 3D models formed from the same contours as in Figure 1. The model that has greater angulation to the *x–z plane* (*right*) now has a greater surface area. *Bottom*, Unshaded versions of the same 3D reconstructions showing the underlying geometry. The ribbons (*a–c*) in the previous figure correspond to the infinitesimally thin lines (*a–c*) in the 3D models. Each pair of lines is connected by a mesh of *small triangles*. Slice thickness is indicated by the separation between the lines with respect to the *z-axis*. The surface area of the 3D model is the sum of the area of the *triangles*.

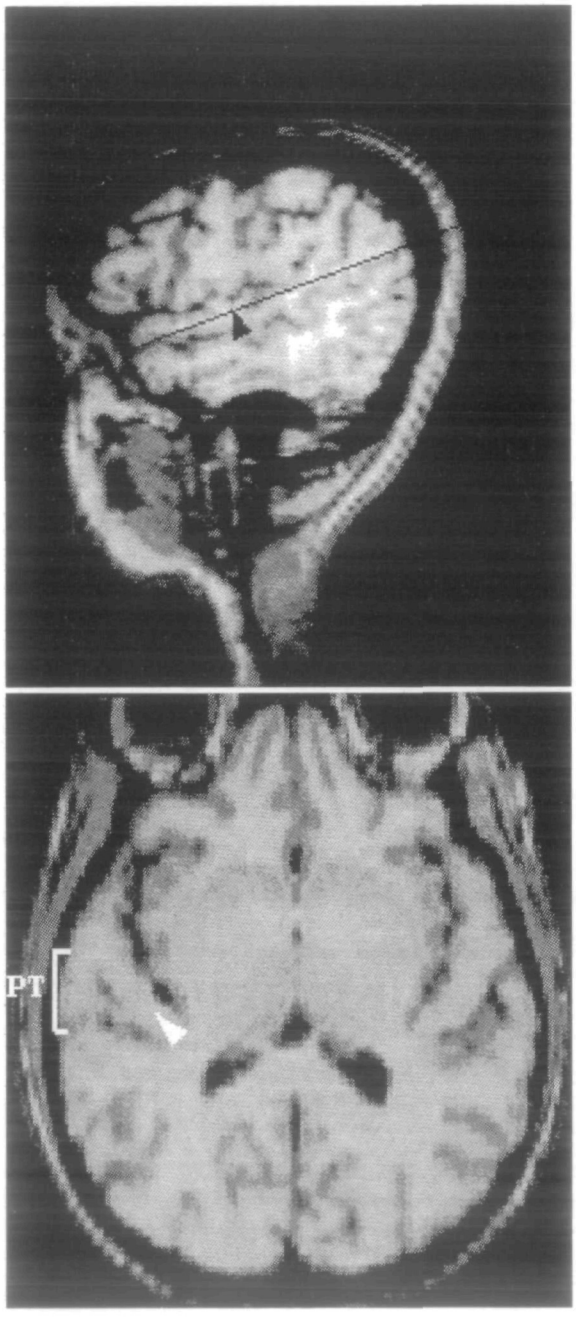


**Figure 3.** Delineation of PT from reformatted images. *Top*, A parasagittal reformation showing HG (*arrowhead*). Anterior is to the left of the image. The angle determined by the caudal edge of HG and the end of the horizontal portion of the fissure (*black line*) is used to define the plane of the PT. *Bottom*, Reformation in the plane of the PT showing HG (*arrowhead*) and the wedge-shaped area of the PT in the left hemisphere. Anterior is at the top of the image. The lateral border of the PT is *bracketed*.

ascending ramus of the sylvian fissure into the supramarginal gyrus. The rostral border is placed at the sulcus posterior to the most anterior transverse gyrus. Thus, any additional HG are included in PT (previous investigators have interpreted the borders of the planum temporale in various ways; for review, see Witelson, 1977; also, Steinmetz and Galaburda, 1991).

The full extent of the caudal infrasylvian surface is designated "cIS." It includes the supratemporal surface posterior to Heschl's gyrus(i) and the superior surface of the supramarginal gyrus lying along the inferior bank of the posterior ascending sylvian ramus (PAR). Rostrally, cIS is identified on coronal sections as the superior surface of the superior temporal gyrus lying lateral and/or caudal to the most posterior HG. When two elevations of gray matter above the superior surface of the superior temporal gyrus appear in the same coronal image, it is difficult to determine if the intervening sulcus extends to the lateral lip of the fissure—the criterion used by Witelson and Pallie (1973) to define whether the caudal elevation is actually a second transverse gyrus. We classify these elevations as extra transverse gyri according to Campain and Minckler's (1976) less stringent criteria and did not include them in cIS. (The anterior border of cIS coincides with the anterior border of PT only if there is a single HG.) Caudally, cIS extends to the posterior tip of the PAR (i.e., the end of the sylvian fissure). This landmark corresponds to the posterior delineation employed in some previous "planum temporale" studies (e.g., Geschwind and Levitsky, 1968; Galaburda et al, 1987; Zilles et al., 1988; Larsen et al., 1989, 1990).

The full extent of the superior temporal region is designated "STR." It includes cIS, the rest of the extra- and intrasulcal surfaces of the superior temporal gyrus and infrasylvian supramarginal gyrus, and HG. STR extended from the most rostral coronal section showing both the superior temporal sulcus and the middle temporal sulcus to the most caudal coronal section showing the PAR.

### *Horizontal Image Reformation and 2D Area Measurement of PT*

The area of PT was measured planimetrically from a reformed horizontal image in the manner of Steinmetz et al. (1989). This was performed in lieu of a 3D measurement, which could not be done because of the difficulty of locating the posterior border of PT in coronal series. First, a parasagittal image that showed HG and the posterior border of PT was reconstructed from the stack of coronals. Second, the reformed sagittal image was used to define the horizontal plane that best captured PT (Fig. 3, top). The angle of this plane was determined by the posterior ridge of HG and the anterior edge of the PAR. A horizontal image was reconstructed from this specification that showed the wedge-like surface of PT (Fig. 3, bottom), which was then measured planimetrically by tracing its outline.

### *3D Surface Area Measurements of cIS and STR*

The surface contour of the cortical mantle was traced with a cursor directly on the coronal MR sections (Fig. 4), which were magnified 3× on the workstation monitor. A triangle mesh that spanned the rostral–caudal gap between adjacent contours (3.0 mm, the section thickness) was interpolated across sections (Fig. 5, bottom). Since the distance between adjacent MR sections was greater than the distance between contour segments within a section, the contours were resampled at a lower resolution so as to mitigate anisotropic

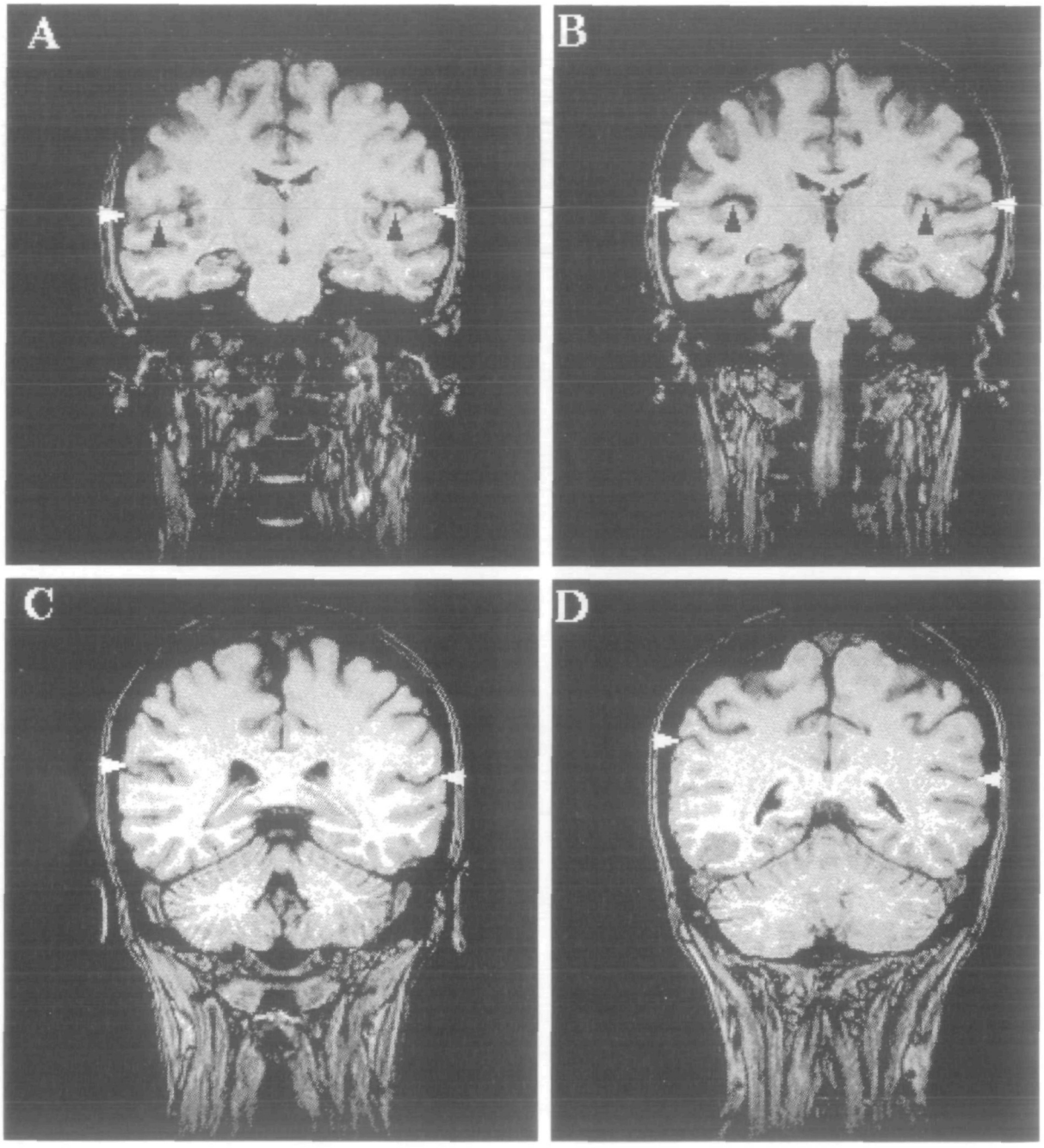


**Figure 4.** Delineation of cIS on coronal images. Four sample images (from a set of 14) used to delineate and measure cIS in one subject. The subject's right is on the left side of the image. The sequence of images *A–D* reflects a rostral–caudal progression. *A*, Demarcation of cIS extends from the lateral ridge of HG (*black arrowheads*) to the lip of the sylvian fissure (*white arrowheads*). *B*, HG appears more medially in successively posterior images. *C*, HG is no longer visible at this level. Demarcation of cIS now extends all the way through the lower bank of the fissure. *D*, The right sylvian fissure appears more elevated than the left at the caudal levels (cf. Habib et al., 1984).

sampling. To avoid aliasing in the contour resampling, points at high curvature were always included in the resampled version.

The area for each triangle was computed by halving the cross product of two of its sides (Fraleigh and Beauregard, 1987). The surface area for the mesh was computed by summing the area of component triangles. In order to minimize error introduced by interpolation across adjacent contours, the triangulation algorithm used a dynamic programming technique (Cormen et al., 1977) to find the mesh between contours with the smallest possible surface area (Fuchs et al., 1977). Hence, a lower bound estimate of surface area was obtained without systematic foreshortening artifacts. Despite differences in hemispheric fissuration, any residual foreshortening would be unlikely to affect one hemisphere more than the other.

### *Quasi-3D Measurements of cIS*

The same coronal contours that were used to estimate cIS in 3D were also used to estimate cIS by (1) multiplying the length of each contour by the thickness

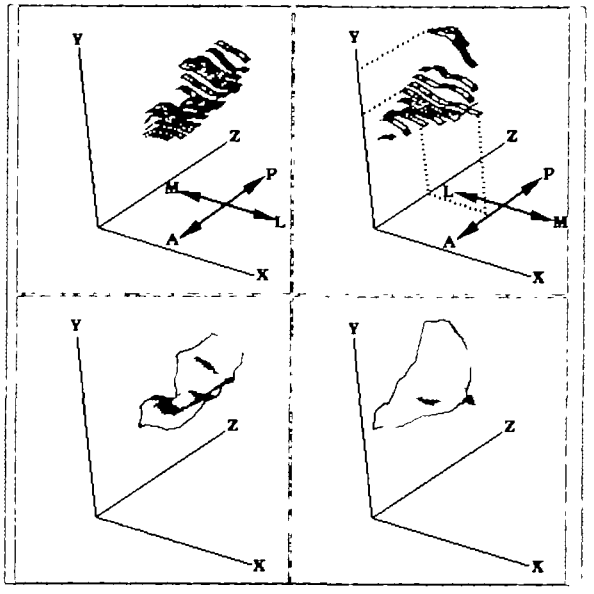


**Figure 5.** Quasi-3D versus 3D models of cIS *Top*, The quasi-3D models of the left and right cIS of one subject *Compass* in the *x–z plane* indicates anterior–posterior and medial–lateral orientations. To aid interpretation, *dotted lines* have been projected from the right hemisphere model onto the *y-axis* and *x–z plane*. Note the disparity in the *y-axis projection* of different contours in the right hemisphere. *Bottom*, Shaded 3D reconstructions based on the same contours at the *top*

of each section in which cIS appeared, and (2) summing across sections. This quasi-3D approach is closely related to flattening the contours onto the plane with a constant spacing and measuring the resulting 2D map planimetrically (Fig. 1). Since gradient information between slices is not used, the underlying representation appears as a series of distinct ribbons, one for each coronal section (Fig. 5, top). The 3.0-mm-thick ribbons correspond to the infinitesimally thin lines that form the sides of each triangle in the 3D model. We did not perform any post hoc corrections of the quasi-3D measures. The distortion of the method, which is related to the angle of elevation between sections, can be reduced by applying a trigonometric correction to the measurement of each section. This is analogous to one flat map technique of increasing the distance between partially straightened contours as a function of their disparity in elevation (Van Essen and Maunsell, 1980), rather than

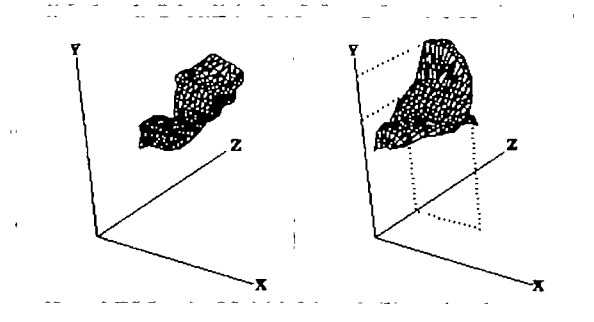


**Figure 6.** The unshaded versions of the 3D reconstructions in Figure 5, showing the underlying geometry of a cIS model. Note how the disparity of contour elevations in the caudal portion of the right cIS results in a mesh of elongated triangles, oriented obliquely to the slice plane.

**Table 1**
2D PT measurements (cm²) and asymmetry coefficients

| Subject | Left | Right | Asymmetry |
|---|---|---|---|
| 1 | 5.30 | 3.66 | −0.366 |
| 2 | 5.03 | 3.98 | −0.233 |
| 3 | 5.95 | 4.69 | −0.237 |
| 4 | 6.10 | 4.95 | −0.208 |
| 5 | 6.70 | 5.38 | −0.219 |
| 6 | 5.04 | 4.22 | −0.177 |
| 7 | 5.72 | 4.04 | −0.344 |
| 8 | 6.95 | 4.29 | −0.473 |
| 9 | 6.31 | 4.19 | −0.404 |
| 10 | 4.31 | 3.93 | −0.092 |
| Mean | 5.74 | 4.33 | −0.275 |
| SD | 0.82 | 0.52 | 0.117 |

keeping a constant spacing between completely straight outlines (e.g., Putnam, 1926; Stensaas et al., 1974; Falzi et al., 1982; Jouandet et al., 1989; Larsen et al., 1989, 1990). In order to perform this correction, the tilt of each section must first be estimated. This may require sampling the angle at many points along individual contours, since the slope of the surface may also vary within a slice plane. The compensation for varying tilt of the surface is incorporated naturally into the 3D approach since the slanted surfaces are explicitly modeled (Fig. 6).

An asymmetry coefficient was computed for all surface area measurements using the formula $(R - L)/(0.5 \cdot (R + L))$, where $R$ is the right surface area in cm² and $L$ is the left surface area in cm². In accordance with previous studies (e.g., Galaburda et al., 1987), a brain with a coefficient magnitude of 0.100 or greater was classified as asymmetric, with a positive value indicating rightward asymmetry and a negative value leftward asymmetry.

## Results

### *PT*

Each subject's surface area estimates and asymmetry coefficients for region PT are listed in Table 1. The surface area of the left PT ranged from 4.31 to 6.95 cm² with a mean and SD of 5.74 ± 0.82. The surface area of the right PT ranged from 3.66 to 5.38 cm² with a mean and SD of 4.33 ± 0.52. The surface area of the left PT was greater than the right for all 10 subjects, and 9 had an asymmetry coefficient with a magnitude of 0.177 or greater. A binomial test showed the distribution of leftward asymmetry (9 of 10) to be significant ($z = 2.53$; $p < 0.02$) (all statistical tests two-tailed). Paired-comparison $t$ tests between the left and right PT also showed a highly significant leftward asymmetry (mean right–left difference = −1.408; $t(9) = 6.83$; $p < 0.0001$). Two subjects had a second HG in both hemispheres, five subjects had a second HG only in the right hemisphere, and one subject had a second HG only in the left hemisphere.

### *cIS*

Each subject's surface area estimates and asymmetry coefficients for region cIS are listed in Table 2. The

**Table 2**
Measures of cIS ($cm^2$) and asymmetry coefficients

| | Quasi-3D | | | 3D | | |
|---|---|---|---|---|---|---|
| Subject | Left | Right | Asymmetry | Left | Right | Asymmetry |
| 1 | 7.23 | 5.62 | −0.251 | 8.45 | 6.99 | −0.164 |
| 2 | 5.94 | 5.32 | −0.110 | 6.83 | 5.72 | −0.047 |
| 3 | 6.18 | 4.89 | −0.233 | 7.28 | 6 59 | −0.209 |
| 4 | 5.90 | 7.31 | 0.215 | 6.74 | 8.14 | 0.250 |
| 5 | 8.64 | 5.75 | −0.402 | 9.15 | 9.97 | −0.004 |
| 6 | 8.31 | 5.16 | −0.468 | 10.85 | 9.70 | −0.446 |
| 7 | 7.44 | 5.32 | −0.332 | 8.20 | 8.55 | 0.073 |
| 8 | 10.58 | 7.09 | −0.394 | 11.85 | 8.45 | −0.302 |
| 9 | 6.12 | 5.50 | −0.107 | 7.25 | 6.64 | −0.021 |
| 10 | 5.51 | 3.70 | −0.393 | 6.46 | 8 99 | 0.563 |
| Mean | 7.18 | 5.57 | −0.248 | 8.31 | 7.97 | −0.031 |
| SD | 1.60 | 1.03 | 0.204 | 1 83 | 1 43 | 0.287 |

data obtained using the 3D model show a mean and SD of 8.31 ± 1.83 for left cIS and 7.97 ± 1.43 for right cIS. Four subjects were leftward asymmetric, four were rightward asymmetric, and two showed no asymmetry. The paired-comparison $t$ test showed no significant asymmetry (mean right–left difference = −0.332; $t(9) = 0.628$; $p = 0.546$).

In contrast, the data obtained using the quasi-3D method showed a leftward asymmetry for nine subjects and a rightward asymmetry for the remaining subject ($z = 2.53$; $p < 0.02$). The mean and SD for the left cIS was 7.18 ± 1.60 and for the right cIS 5.57 ± 1.03. The paired-comparison $t$ test showed a significant leftward symmetry (mean right–left difference = −1.62; $t(9) = 3.515$; $p = 0.007$).

Since the same contours were used for both 3D and quasi-3D surface area estimates, the different results obtained concerning hemispheric asymmetry were solely due to differences in the algorithms. Analysis of the pairwise differences of the two algorithms (3D vs quasi-3D surface area) showed significantly smaller estimates for both left and right cIS surface area (Fig. 7), with worse underestimation on the right (left: mean difference = 1.123; $t(9) = 6.473$; $p < 0.0001$; right: mean difference = 2.408; $t(9) = 4.347$; $p = 0.002$). The magnitude of the underestimation is also more variable in the right (SD of difference: left, 0.549; right, 1.752). In some cases, the surface is grossly underestimated on the right, which reflects an extreme obliquity of the PAR relative to the coronal plane.

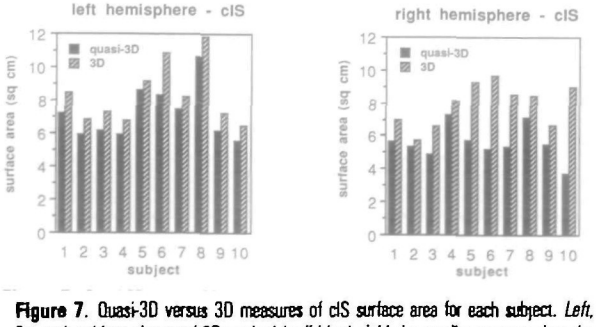


**Figure 7.** Quasi-3D versus 3D measures of cIS surface area for each subject. *Left*, For each subject, the quasi-3D method (*solid bar*) yielded a smaller measure than the 3D method in the left hemisphere. *Right*, Quasi-3D estimates were also significantly smaller for the right hemisphere. However, the distortion (reflected by the disparity in the *height* of pairs of *solid* and *hatched bars*) is much greater in the right hemisphere than in the left.

### *STR*

Each subject's surface area estimates and asymmetry coefficients for region STR are listed in Table 3. The surface area of the left STR ranged from 22.28 to 36.28 $cm^2$ with a mean and SD of 29.81 ± 4.74. The surface area of the right STR ranged from 21.26 to 32.67 $cm^2$ with a mean and SD of 29.29 ± 4.05. Leftward asymmetry was found for four subjects, rightward asymmetry for three subjects, and no asymmetry for three subjects. Paired-comparison $t$ tests between the left and right STR showed no asymmetry (mean right–left difference = −0.525; $t(9) = 0.429$; $p > 0.67$).

## Discussion

We found no hemispheric asymmetry involving the combined surface area of the superior temporal gyrus, HG, and the infrasylvian supramarginal gyrus. When the analysis was restricted to the cortical surface lying caudal to HG along the inferior bank of the sylvian fissure (including the PAR), again no asymmetry was found. This same surface was then measured using a

**Table 3**
3D measures of STR ($cm^2$) and asymmetry coefficients

| Subject | Left | Right | Asymmetry |
|---|---|---|---|
| 1 | 31 46 | 32.67 | 0.038 |
| 2 | 31.13 | 32.16 | 0.033 |
| 3 | 36.28 | 31.88 | −0.129 |
| 4 | 27.40 | 21.26 | −0.252 |
| 5 | 36.28 | 31.88 | −0.129 |
| 6 | 22.28 | 26.07 | 0.157 |
| 7 | 27.06 | 24.39 | −0.104 |
| 8 | 25.64 | 28.51 | 0.106 |
| 9 | 26.71 | 31.82 | 0.175 |
| 10 | 33.88 | 32.23 | −0.050 |
| Mean | 29.81 | 29.29 | −0.016 |
| SD | 4 74 | 4.05 | 0.140 |

quasi-3D method that failed to take into account the folding and curvature of the cortical surface across adjacent coronal sections. As expected, significantly smaller surface area estimates were obtained using the quasi-3D method. Because the tilt of the ascending ramus is greater on the right than on the left, foreshortening artifact affected the right more than the left. As a result, the quasi-3D method yielded spurious leftward asymmetry. The possibility that the 3D surface area estimates failed to show the expected asymmetry because of anomalous laterality effects in our subjects was ruled out by replicating the findings of Steinmetz et al. (1989) with respect to PT asymmetry.

The distortions engendered by the quasi-3D method may be exaggerated compared to those of other studies that carefully control the angle of anatomical section (e.g., Larsen et al., 1989) or photographic plane (e.g., Witelson and Pallie, 1973; Galaburda et al., 1987). However, when the region of interest in one hemisphere is more concave (or convex) than the corresponding region in the other hemisphere, assessment of hemispheric asymmetry cannot be completely eliminated unless a 3D approach is used. The greater the folding of the surface, the greater will be the foreshortening artifact, and the greater the advantage of carrying out surface area estimates in 3D. The 3D approach also obviates trigonometric corrections that require sampling the tilt along the cortical surface within each section in order to calculate a correction factor.

One disadvantage of the present procedure is that it can only be carried out on planar contours. Consequently, sulci that run parallel to the slice plane may be underrepresented in the 3D model. Reconstruction techniques that do not rely on contours, such as the "marching cubes" algorithm of Lorensen and Cline (1987) and the 3D shrink wrap method (Sereno and Dale, 1992; Dale and Sereno, 1993), may produce models of cortical geometry with even higher fidelity.

The pattern of asymmetry of the PT and overall symmetry of the caudal infrasylvian region supports the claim that leftward asymmetry of the PT is "balanced" by rightward asymmetry of the infrasylvian supramarginal gyrus (Steinmetz et al., 1990; Witelson and Kigar, 1992). The possible functional significance of the (a)symmetry, if any, can be debated. The frequency of leftward asymmetry has been low compared with the estimate of left hemisphere language dominance in the general population. This is a problem for theories of structural asymmetry underlying functional asymmetry. However, measurements restricted to the PT (as defined in the present study) may reveal a greater proportion of leftward asymmetry than previous parcellations that have included some parietal tissue, though two recent studies relating quantitative measures of the isolated temporal bank to handedness in the same subjects have not yielded a consistent pattern of results (Steinmetz et al., 1991; Witelson and Kigar, 1992). Yet another interpretation is that the asymmetry of the PT is a side effect of the more anterior upswing of the sylvian fissure on the right rather than a manifestation of functionally significant increase in size on the left.

While these data may not support a characterization of language dominance as simply an increase in the sheer amount of cortex in one hemisphere (Gazzaniga, 1992), it does not necessarily mean that the trend toward increased angulation of the right posterior sylvian fissure (which is reflected by the larger left PT) is unrelated to functional asymmetry. This is supported by *in vivo* studies correlating functional asymmetries of handedness (LeMay and Culebras, 1972; Hochberg and LeMay, 1975; Kertesz et al., 1986) and language lateralization (Ratcliff et al., 1980) with various anatomic asymmetries in the temporoparietal region. An alternative hypothesis (Steinmetz and Galaburda, 1991) is that gross morphological differences and cerebral dominance may both be consequences of a third unknown factor. Investigations into microcircuity of auditory association cortex (Seldon, 1982) and the dynamics of cortical growth and fissurization (Chi et al., 1977a; Welker, 1990) may provide insights in this regard.

## Notes

This investigation was supported by Office of Naval Research Grant N00014-89-J-3035, NIH/NINDS PO1 NS17778-10, NIDOCD K08-DC00071, the James S McDonnell Foundation, the Sackler Foundation NARSAD, and Mr. and Mrs. James Winston. We thank Prof Scot Drysdale for guidance on the application of dynamic programming to surface tessellation; Prof. David Mumford for a helpful discussion of surface area distortions; Dr. Susan Chipman, who initially suggested this approach; Drs. Albert Galaburda, Sandra Witelson, and Debra Kigar for informative discussions; and Jeff Hutsler, Dr. Robert Knight, and Dr. Helmi Lutsep for helpful comments and criticisms concerning earlier drafts of the manuscript. Some of these results were presented at the 22nd annual meeting of the Society for Neuroscience held in Anaheim, CA, October, 1992.

Correspondence should be addressed to William Loftus, Center for Neuroscience, University of California, Davis, CA 95616

## References

Campain R, Minckler J (1976) A note on the gross configurations of the human auditory cortex. Brain Lang 3:318–323.

Chi JG, Dooling EC, Gilles FH (1977a) Gyral development of the human brain. Ann Neurol 1:86–93.

Chi JG, Dooling EC, Gilles FH (1977b) Left–right asymmetries of the temporal speech areas of the human fetus. Arch Neurol 34:346–348.

Cormen TH, Leiserson CE, Rivest RL (1990) Introduction to algorithms. Cambridge, MA: MIT Press

Dale AM, Sereno MI (1993) Improved localization of cortical activity by combining EEG and MEG with MRI cortical surface reconstruction: a linear approach. J Cognit Neurosci 2:162–176

Falzi G, Perrone P, Vignolo LA (1982) Right–left asymmetry in anterior speech region. Arch Neurol 39:239–240.

Fraleigh JB, Beauregard RA (1987) Linear algebra Reading, MA: Addison-Wesley.

Fuchs H, Kedem KD, Uselton SP (1977) Optimal surface reconstruction from planar contours. Graphics Image Process 20:693–702.

Galaburda AM, Corsiglia J, Rosen GD, Sherman GF (1987)

Planum temporale asymmetry, reappraisal since Geschwind and Levitsky. Neuropsychologia 25:853–868.
Gazzaniga MS (1992) Nature's mind. New York: Basic.
Geschwind N, Levitsky W (1968) Human brain: left–right asymmetries in temporal speech region. Science 161:186–187.
Habib M, Renucci RL, Vanier M, Corbaz J-M, Salamon G (1984) CT assessment of right–left asymmetries in the human cerebral cortex. J Comput Assist Tomogr 8:922–927.
Hochberg FH, LeMay M (1975) Arteriographic correlates of handedness. Neurology 25:218–222.
Jouandet ML, Tramo MJ, Herron DM, Hermann A, Loftus WC, Bazell J, Gazzaniga MS (1989) Brainprints: computer-generated two-dimensional maps of the human cerebral cortex *in vivo* J Cognit Neurosci 1:88–117.
Kertesz A, Black SE, Polk M, Howell J (1986) Cerebral asymmetries on magnetic resonance imaging. Cortex 22:117–127.
Larsen JP, Ødegaard H, Grude TH, Høien T (1989) Magnetic resonance imaging—a method of studying the size and asymmetry of the planum temporale Acta Neurol Scand 80:438–443.
Larsen JP, Høien T, Lundberg I, Ødegaard H (1990) MRI evaluation of the size and symmetry of the planum temporale in adolescents with developmental dyslexia. Brain Lang 39:289–301.
LeMay M, Culebras A (1972) Human brain—morphologic differences in the hemispheres demonstrable by carotid angiography. N Engl J Med 287:168–170.
Leonard CM, Voeller KKS, Lombardino LJ, Honeyman JC, Agee OF (1992) What is anomalous in the dyslexic planum? Soc Neurosci Abstr 18:331.
Lorensen WE, Cline HE (1987) Marching cubes: a high resolution 3D surface construction algorithm. Comput Graphics 21:163–169.
Nass RD, Gazzaniga MS (1987) Cerebral lateralization and specialization in human central nervous system. In: Handbook of physiology, Vol 5, The nervous system, Pt 1, Higher functions of the brain (Mountcastle VB, Plum F, Geiger SR, eds), pp 701–761. Bethesda, MD: American Physiological Society.
Oldfield RC (1971) The assessment and analysis of handedness: the Edinburgh inventory. Neuropsychologia 9:97–113.
Putnam TJ (1926) Studies on the central visual system: the details of the organization of the geniculostriate system in man. Arch Neurol 16:683–704.
Ratcliff G, Dila C, Taylor L, Milner B (1980) The morphological asymmetry of the hemispheres and cerebral dominance for speech: a possible relationship. Brain Lang 11:87–98.
Rubens AB, Mahowald MW, Hutton T (1976) Asymmetry of the lateral (sylvian) fissures in man. Neurology 26:620–624.
Seldon HL (1982) Structure of human auditory cortex. III. Statistical analysis of dendritic trees. Brain Res 249:211–221.
Sereno MJ, Dale AM (1992) A technique for reconstructing and flattening the cortical surface using MRI images Soc Neurosci Abstr 18:585.
Steinmetz H, Galaburda AM (1991) Planum temporale asymmetry: *in-vivo* morphometry affords a new perspective for neuro-behavioral research. Reading Writing 3:331–343.
Steinmetz H, Rademacher J, Huang Y, Hefter H, Zilles K, Thron A, Freund H-J (1989) Cerebral asymmetry: MR planimetry of the human planum temporale. J Comput Assist Tomogr 13:996–1005.
Steinmetz H, Rademacher J, Jäncke L, Huang Y, Thron A, Zilles K (1990) Total surface of temporoparietal intrasylvian cortex: diverging left–right asymmetries. Brain Lang 39:357–372.
Steinmetz H, Volkmann J, Jäncke L, Freund H-J (1991) Anatomical left–right asymmetry of language-related temporal cortex is different in left- and right-handers. Ann Neurol 29:315–319.
Stensaas SS, Eddington DK, Dobelle NH (1974) The topography and variability of the primary visual cortex in man. J Neurosurg 40:747–755.
Teszner D, Tzavaras A, Gruner J, Hécaen H (1972) L'asymetrie droite-gauche du planum temporale: a propos de l'etude anatomique de 100 cerveaux. Rev Neurol 126:444–449.
Van Essen DC, Maunsell JHR (1980) Two dimensional maps of the cerebral cortex. J Comp Neurol 191:255–281.
von Economo C, Horn L (1930) Über windungsrelief, maße und rindenarchitektonik der supratemporalfläche, ihre individuellen und ihre Seitenunterschiede. Z Neurol Psychiatr 130:678–757.
Wada J, Clarke R, Hamm A (1975) Cerebral hemispheric asymmetry in humans: cortical speech zones in 100 adult and 100 infant brains. Arch Neurol 32:239–246.
Wechsler D (1981) Wechsler Adult Intelligence Scale—revised. New York: Psychological Corporation.
Welker W (1990) Why does cerebral cortex fissure and fold? A review of determinants of gyri and sulci. In: Cerebral cortex, Vol 8B, Comparative structure and evolution of cerebral cortex, Pt II (Jones EG, Peters A, eds), pp 3–136. New York: Plenum.
Wernicke C (1874) The symptom complex of aphasia. Reprinted in: Diseases of the nervous system (Church A, ed), pp 265–324. New York: Appleton, 1908.
Witelson SF (1977) Anatomic asymmetry in the temporal lobes: its documentation, phylogenesis, and relationship to functional asymmetry. Ann NY Acad Sci 299:328–354.
Witelson SF, Kigar DL (1991) Anatomy of the planum temporale in relation to side, handedness, and sex. Soc Neurosci Abstr 17:1044.
Witelson SF, Kigar DL (1992) Sylvian fissure morphology and asymmetry in men and women: bilateral differences in relation to handedness in men. J Comp Neurol 323:326–340
Witelson SF, Pallie W (1973) Left hemisphere specialization for language in the newborn: neuroanatomical evidence of asymmetry. Brain 96:641–646.
Zilles K, Armstrong E, Schleicher A, Kretschmann H-J (1988) The human pattern of gyrification in the cerebral cortex. Anat Embryol (Berl) 179:173–179.